Silicon (2023) 15:571–581
https://doi.org/10.1007/s12633-022-02015-9

ORIGINAL PAPER

Critical Examination of the Role of Silica Nanoparticle Dispersions in Heat Transfer Fluid for Solar Applications

Dinesh Babu Munuswamy[1] · Yuvarajan Devarajan[2]

Received: 11 March 2022 / Accepted: 4 July 2022 / Published online: 30 July 2022

Abstract
Silica nanoparticles are eco-friendly with high heat transfer potential due to their low-cost synthesis, abundant natural resources, and mass production. Silica nanoparticles with advantages such as biocompatibility, ease-of-functionalization, and large surface area are widely employed in solar applications. Silica nanoparticles possess excellent properties such as good photoconductivity, ideal thermal expansion, high corrosion resistance, and long-term durability, which improve the system's overall efficiency. Dimethyldichlorosilane was employed to prepare silica nanoparticles into hydrophobic nanoparticles. The titration method computed the hydroxyl number of silica nanoparticles and reduced it after modification. The novelty of this work is to enhance the overall efficiency of the solar water heater by adding silica nanoparticles in heat transfer fluid owing to its higher thermal stability, heat resistance and improved structural properties of the nanoparticle. This work reveals a detailed study on the effect of silica nanoparticles on the performance parameters of the solar water heater. Silicon nanoparticles are dispersed with water using NaOH for pH adjustments and Cetyl Triammonium Bromide (CTAB) (1% by wt) as the dispersant to accelerate the vaporization and heating of the medium by local nanoscale heating. This study proposes that incorporating silica nanoparticles at different mass fractions shall improve the s overall efficiency of solar collectors. Silica nanoparticles are dispersed into water with and without using surfactant inside the absorber riser tubes for different mass fractions. The efficiency of the solar flat plate collector is calculated using the ASHRAE method. A collector of the area of 0.5 m^2 of 25 LPD has been envisioned and made up with necessities to insert T-type thermocouples to study the temperature distribution. The weight fractions used are 0.2%, 0.4%, and 0.8%, and the experimental results showed an improved heat transfer was pragmatic in the collector using nanoparticles. The efficiency of the solar collector is improved by 2.5, 5.1 and 8.4% by adding Silicon dioxide nanoparticles at 0.2%, 0.4%, and 0.8% weight fractions, respectively. This study concludes that silicon oxide possesses high heat transfer potential and shall be employed in thermal systems.

Keywords Silicon dioxide · Nanoparticles · SiO_2 Nanofluid · Collectors · Efficiency

Nomenclature

LPD	Litres Per Day
SiO_2	Silicon dioxide
TiO_2	Titanium dioxide
MWCNT	Multi-Walled Carbon Nanotubes
Al_2O_3	Aluminium Oxide
ZnO	Zinc oxide
MgO	Magnesium Oxide
CeO_2	Cerium Oxide
CTAB	Cetyl Triammonium Bromide
SFPWHS	Solar Flat Plate Water Heater System
FPC	Flat Plate Collector
CNC	Crystal Nano Cellulose
CNT	Carbon Nano Tube
SWCNT	Single-Walled Carbon Nano Tube

1 Introduction

The environmental degradation of renewable energy and its storage system led the researchers to design a new energy storage system efficiently. The energy system has to be designed and maintained to ensure the waste of energy that can be utilized for other industrial and domestic needs brainstorming process yielded several ideas for improving the

✉ Yuvarajan Devarajan
dyuvarajan2@gmail.com

[1] Department of Mechanical Engineering, Panimalar Engineering College, Poonamalle, Chennai 600123, India

[2] Department of Thermal Engineering, Saveetha School of Engineering, SIMATS, Chennai, Tamilnadu, India

performance of the solar flat plate collector system. In the face of many other options, we decided to replace plain copper tubes with internally finned or grooved ones. Spiraling fins or grooves line the tube's interior surface. Consequently, the tube's heat transfer rate is higher than a plain tube, meeting the same specifications.The high internal surface area of contact and turbulent liquid flow increases the heat transfer rate (efficiency) [1]. The system's performance is increased when the collector temperature rises due to increased heat transfer. As a result, a smaller unit can be produced to meet the same specifications [2]. Utilizing nanofluids in solar thermal collectors presents several beneficial opportunities for improvement [3]. Some advantages include increased thermal efficiency, a possible reduction in collector size, and improved economic and environmental performance [4]. However, the performance and predictability of nanofluids in collectors are still subject to several restrictions. The applications of nanoparticles are growing rapidly. Among them are materials such as silicon dioxide. Its use has advantages: high adsorption capacity, low toxicity, easy synthesis, and inexpensive. Nanoparticles enhance the thermophysical properties such as thermal conductivity and specific heat capacity of nanofluids in heat transfer applications. Cost reduction of an SFPWHS can be achieved either by using low-cost material (longevity decreases) or reducing the collector area. Altering the collector area can be possible by enhancing the heat transfer rates. Abu Shadate Faisal Mahamude et al. [5] examined the CNC and graphene hybrid fluid with a volumetric fraction of 0.5 percent at 80 °C, improved thermal conductivity, viscosity, and other parameters. CNC and graphene hybrid nanofluid can outperform a conventional base fluid thermally. Ashour et al. [6] investigated that usage of H_2O–CuO nanofluid has the highest average efficiency at a mass flow rate of 0.0125 kg/s for a volume fraction of 0.15%, similarly for H_2O–ZnO nanofluid had an average efficiency of 77.64%, compared to water is 60.21%.. Shirin Rostami et al. [7] investigated the heat transfer characteristics of flat plate solar thermal collectors with circular and elliptical serpentine designs. The result showed under turbulent flow; elliptical cross-section thermal efficiency reaches 56%. Hossein et al. [8] found that the SWCNT-CuO/water and MWCNT-CuO/water heat transfer coefficients increased by 8 and 4.1% compared to H_2O at Reynolds 10,000.Abu-Hamdeh et al. [9] The results showed increased TiO_2/SiO_2 nanofluid's thermal conductivity and efficiency, proving its high potential in energy systems. Farhana et al. [10] examined that using 0.5% Al_2O_3 and 0.5% CNC nanofluids increased solar collector efficiency by 2.48% and 8.46%, respectively. Bakhtiari et al. [11] the study examined TiO_2-Graphene/Water hybrid nanofluid thermal conductivity. At 25 to 75 °C and different volume fractions, hybrid nanofluids were tested (0.005 to 0.5%). At 0.5% volume fraction and 75 °C, thermal conductivity was 27.84% higher than the base fluid. Ahmadi et al. [12] and Gorjian et al. [13] Studied that flat plate collectors collect energy from the sun and convert it to thermal energy. Vengadesan and Senthil [14] employed active and passive methods to augment heat energy at the receiver end for absorber tubes to be properly utilized, increasing the effectiveness. Hussein et al. [15] investigated Tripartite hybrid nanofluids added with a surfactant of Tw-80 and examined the collector efficiency for three different volume flow rates of 2 L/min, 3 L/min, and 4 L/min. The results showed that a volume rate of 4 L/min with maximum efficiencies of 85% is achieved using hybrid nanofluids. Moravej et al. [16] investigated using TiO_2/H_2O nanofluid experimentally compared to H_2O as working fluids in a symmetrical four-sided absorber collector system. The collector shows a determined 78% efficiency when 1% wt. fraction of TiO_2/H_2O. Mohamed et al. [17] conducted experiments using ZnO nanoparticles with 23 nm of 0.05 vol% and 0.1 vol% and base working fluid water. The result showed that thermal energy increased by 3.36% and 7.78% for 0.05 vol% and 0.1 vol% Similarly, the efficiency arrived at nearly 4.81% and 6.57% for water used. Tong et al. [18] examined the efficiency of absorbing solar collector system for different nanofluids were verified for working fluids the maximum efficiency arrived is for MWCNTs nanofluid 0f 87% and lowest arrived is for the water of 62%. (Dinesh babu et al., 2020) [19] studied experimentally for two different types of collectors, one internally finned riser tubes collector and another with unfinned tube collector subjects to two different nanofluids of Al_2O_3 and CuO nanofluids. After testing, internally finned tube collectors were observed using a 0.4% weight fraction for Al_2O_3 nanofluid efficiency of nearly 7.8% to unfinned tube collectors. Hajabdollahi et al. [20] studied that usage of SiO_2/H_2O nanofluid with a lower percentage by volume shows a better efficiency when compared to that of Al_2O_3/H_2O and SiO_2/H_2O nano-fluids on an annual cost reduction of 27.88% when SiO_2/H_2O for an efficiency of 56.4%. Mondragon [21] studied that due to the deposition of Al_2O_3-H_2O nanoparticles, there is a decrement in efficiency from 47% to 41.5% and heat removal factor. Tong et al. [22] investigated using Al_2O_3/H_2O for a volume percentage of 0.01%. The efficiency attained was 77.5%, 21.9% for water. Besides, the absorber using SiO_2/H_2O exhibited an all-out efficiency of 73.9%. Mirzaei et al. [23] Studied experimentally using SiO_2-H_2O nano-fluids with 0.1 vol% of 40 nm were prepared as working fluids inside the absorber tubes for mass flow rates were in the range of 1, 2, and 4 L/min. The thermal efficiencies of the absorber increased by 15.2%, 17.1%, and 55.1% for SiO_2-H_2O compared to that of H_2O. Arora et al. [24] studied using Al_2O_3-H_2O nanoparticles of 20 nm for a volume fraction of 0.1%. The maximum peak thermal efficiency attained is 83.17% for a collector absorber area of $2m^2$. Dehaj and Mohiabadi [25] investigated for absorber collector area of $4m^2$

using MgO-water nanofluid for a volume fraction of 0.014 – 0.032% at a mass flow rate of 14L/min. The efficiency attained for MgO -water-based nanofluid is 77% and for base working fluid water is 69%. Jouybari et al. [26] experimentally studied a colletor area of 0.6m^2 using SiO_2 -H_2O of 20-30 nm particle size for a volume fraction of 0.4—0.6 vol% the heat removal factor 0.4% reduced by 55.2% and for 0.6% is 51.7%. Mirazaei et al. [27] tested a collector area of 1.51m^2 using Al_2O_3/H_2O for a 0.1%weight fraction. The results showed a thermal efficiency increased nearly to 23.6%. Syam Sundar et al. [28] studied using Al_2O_3-H_2O for a particle size of < 20 nm of area 2m^2 for a volume fraction of 0.3%. The results showed an increase in the collector efficiency along with an increase in Re. Jouybari et al. [29] experimentally studied using SiO_2-H_2O nanoparticles of size 20-30 nm for 0.2%, 0.4%,and 0.6% thermal performance achieved nearly about8.1% efficiency for absorber area of $90\times20\times7$ $X10^{-6}$ m^3. Stalin et al. [30] investigated a collector absorber area of 2m^2 using CeO_2 -H_2O of 20 nm for 0.01%by volume. The collector has reached nearly 78.2% efficiency. Dinesh babu et al. [31] experimentally investigated using three different nanofluids of aluminium, copper, and Zirconium nano-fluids are tested for thermal efficiency. The result showed that alumina nanofluid for 0.4% wt. fraction showed that alumina nanofluid had a superior efficiency for the collector side of 17% related to the base working fluid water. Dinesh babu et al. [32] investigated a collector area of 945×420 mm for two collectors for internal fin and conventional collectors subjected to different weight fractions of Al_2O_3-H_2O nano-fluids and water. Results showed a maximum efficiency attained for 0.4% weight fraction of Al_2O_3 for finned tube collector of nearly 74.81% to that unfinned tube collector of 71.43%. This shows that the doping of nano-fluids augments the transfer of heat, increasing the overall efficiency of the collector system. Faizal et al. [33] tested a collector area of 1.84m^2 using SiO_2-H_2O nanoparticles for varying mass fractions. A better option is that adding the phase change material will influence better heat transfer rate when used internally inside the riser tubes. The result showed the efficiency of the flat plate collector was enhanced by 23.5% for 0.2%. It is also relevant to note that these losses do increase with the increase in temperature of the working fluid.

2 Experimental Setup

With the superior performance of finned tube SFPWHS over conventional SFPWHS, it was envisaged to fabricate the designed system and carry out experimental investigations. Accordingly, a double loop system was fabricated so that the nanoparticles-laden water will absorb solar energy in the collector (primary loop) and transmit it to the water in the storage tank through the secondary loop. Both the loops were designed to be of ladder-type construction. A solar flat plate collector is a fabricated dual circuit consisting of primary and secondary circuits with 2.5 and 25 L, respectively. The absorber tubes are fabricated with four riser tubes arranged parallel with a 12 mm outer diameter of 1000 mm in length, soldered for a 0.5 m^2 absorber plate. All the riser tubes are connected in a 1" main inlet header, and the outlet point is connected with a 1" main outlet header. The main outlet header is connected to the ladder-type heat exchanger's inlet and the main header(inlet) collector. Two vents are provided in the primary circuit, one for loading the nanofluid and the other for venting the primary circuit. The storage tank has a 25-L capacity with an inlet, outlet, and vent header. A ladder-type heat exchanger separates the storage tank and collector side to enhance heat transfer in storage fluid.

2.1 Silicon Nanoparticle

The nanoparticle SiO_2 was prepared and operated in Solar Collector at different weight fractions of 0.2%, 0.4%, and 0.8% with and without surfactant. Hence required weight fraction of the nanoparticle is dispersed in 2.5 L of distilled water and then mixed by a magnetic stirrer, followed by sonification for better distribution in the base fluid. Figure 1. shows the experimental setup of the solar water heater, and the reason for the selection of nanoparticles is shown in Fig. 2.

3 Instrumentation Setup

The primary circuit of 25 LPD solar Flat plate collectors contains four parallel 12 mm tubes connected in 1inch main inlet and outlet headers. To monitor the temperature profile

Fig. 1 Experimental set-up of solar water heater

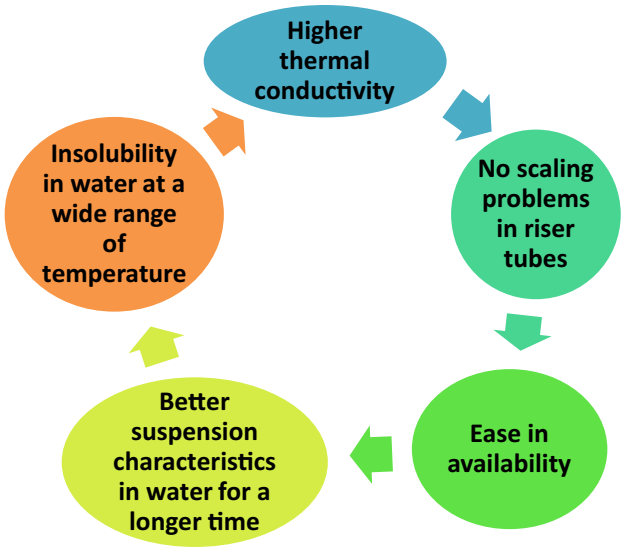

Fig. 2 Selection of SiO_2 nanoparticles

and flow distribution across the tubes at different lengths of the riser tube, The T-type thermocouples are brazed on the surface of the riser tube. Two T-type thermocouples are installed in the main header, one at the inlet and the other at the outlet of the riser tube, to monitor the total temperature change across the primary circuit of the collector. To understand the natural convection thermosyphon effect and pressure drop across the collectors, pressure gauges range from 0- 1 bar installed at the inlet and outlet of the main header of the primary circuit. A heat exchanger with the maximum surface is brazed in the primary circuit to enhance the heat transfer rate between the primary and secondary circuits. Figure 3 shows the instrumentation setup for the designed solar collector. A WATCH-DOG Annemometer (Fig. 4) was used to measure air velocity, insolation, Relative Humidity, Dew Point Temperature, and Ambient Temperature. The temperature readings are logged using the Agilent data logger system shown in Fig. 5.

Fig. 3 Instrumentation set up solar water heater

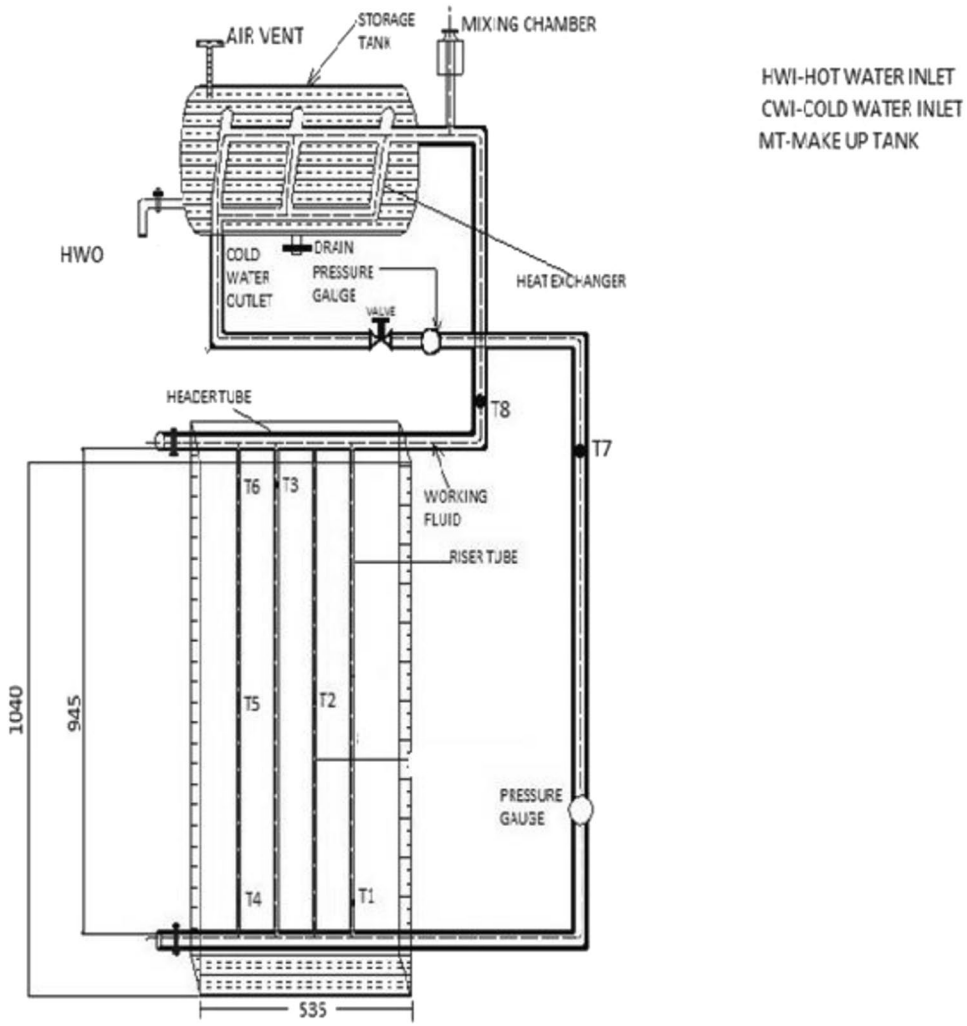

Fig. 4 Watch dog anemometer

Fig. 5 Agilent data logger

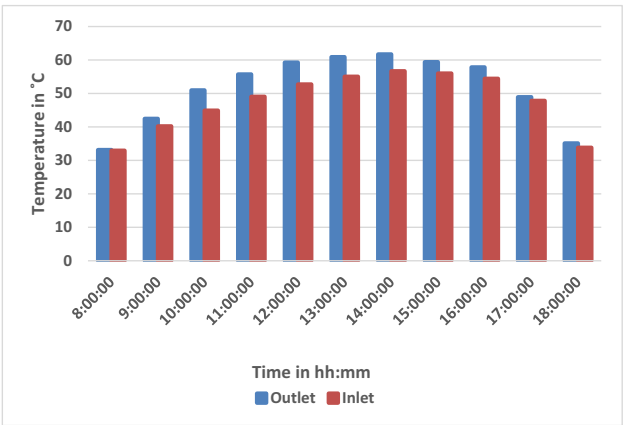

Fig. 6 Time (h) vs inlet temp (C) and outlet temp (C) for base fluid

4 Results and Discussion

4.1 Baseline Data with the Base Fluid

Temperature and efficiency are used to improve flat plate water heating systems. The collectors have four riser tubes, so thermocouples were placed at the top (T6), middle (T5), and bottom (T4). Thermowells were used to measure water temperature without solar insolation affecting thermocouples. All riser tubes should be arranged similarly. More thermowells would hinder water thermo-siphoning. So, one thermowell per riser tube was added. This thermowell is parallel to the last riser tubes. T3 parallel to T6, T2 to T5, and T1 to T4. These arrangements revealed the temperature profile across flat plate collector riser tubes and allowed flow analysis. The heat transfer fluid (water) absorbs the heat in the thermal system and leaves it at an elevated temperature. The outlet temperature rises quickly at about 7:30 am, reaches its peak at 2:00 pm, and then decreases owing to a reduction in insolation. From 11 am to 2 pm, there is a 5 °C difference between the output and input temperature. Figure 6 shows the inference between time (h) vs Inlet Temp (°C) and Outlet Temp (°C) for water. Three pairs of thermocouples are fixed at different heights on the tubes running inside the collector. Temperature plots of these pairs (T1 and T4, T2 and T5, T3 and T6) reveal that the temperatures at all the tubes at the same height are the same for accuracy. This shows a uniform flow of water through all tubes since water is the medium that carries away the heat of the tubes.

A thermocouple was fixed at the tank's top, middle and bottom positions. The average of these temperatures gives the temperature of the tank. As expected, the top layer was warmer than the middle layer. But this trend changed after 10 am when the middle and bottom layers recorded the same temperature. However, after 5 pm, the original trend was observed. Solar radiation warms the body where it falls. In this instance, the fins are heated, and heat is transferred to the water via tubes. The air around the fins achieves a higher temperature than the fins. There is a natural convection movement inside the collection unit's entrapped air [34]. From 10 am to 1 pm, there is a 4˚C temperature differential between the fins and the air gap.

4.2 Baseline Data with SiO_2 Nanofluid

SiO_2 nano-fluids are prepared with different weight fraction increases due to the surface tension, viscosity, and other flow characteristics such as Reynolds number changes, leading to a higher pressure drop in the collector, which results in a breaking of thermosyphons. Silicon dioxide nanoparticles are operated for different weight fractions in the 25 LPD Solar flat plate collector. The results, such as the temperature profile of the riser tube, heat gained, and its efficiencies, are compared based on working in the fluid. The test was performed in Tamil Nadu, Chennai (India) on a bright sunny day with a clear sky of the average ambient temperature of a maximum of 35℃, wind velocity of 6 m/s, and relative humidity of 74%. Additionally, prolonged aggregation raises the fluid's viscosity, lowering the flow rate in thermosyphons and raising the pump power needed in forced convection systems [35]. Both of these factors will, in the long run, bring the system's efficiency down. In many heat transfer systems, the thermal performance of nanofluid is superior to that of conventional heat transfer fluid. However, some limitations still exist in evaporative systems such as heat pipes.

Silicon nanofluid with a mass fraction of 0.2% is compared against the instantaneous insolation for a particular day to determine the fluctuation of storage tank temperature on a given day. The graph displays the insolation levels from midnight to three in the afternoon. At midnight, the temperature of the storage tank drops to roughly 35˚C. With rising sun insolation beginning at 6 am, the temperature of the storage tank rises steadily until noon, levels out at 2 pm, and remains at roughly 50˚C until 3 pm. Temperature sensors are situated at the same height on different riser tubes. Silicon oxide nanofluid is compared against the day's instantaneous insolation to determine the daily temperature change of storage tanks. At midnight, the temperature of the storage tank drops to roughly 35˚C. With rising sun insolation beginning at 6 am, the temperature of the storage tank rises steadily until noon, levels out around 2 pm, and remains at roughly 55 °C until 3 pm. Compared to the data for the 0.2% mass fraction, the peak temperature of the storage tank is about 5 °C higher.

4.3 Thermal Stratification in Storage Tank with Water

Figure 7 shows the temperature variations of the storage tank's top, middle and bottom layers concerning time. Based on the heat transfer area and insolation values received by the working fluid from the absorber plate, transfer the collected heat energy into the secondary side of the collector. Thermal stratification inside the secondary side depends on the heat transfer area of ladder-type heat exchanger heat effectiveness. Figure 7 reveals that the average tank temperature rises for 15 h and falls due to lower insolation values and heat loss to the surroundings because of the reverse heat flow from the storage tank to the ambient.

The heat gained by the storage tank is mainly based on the temperature difference (driving force) in primary and insolation values, heat loss coefficient, and heat removal factor for every 5 min of operation. Figure 8(a and b) represents the collector's heat input and energy balance. Heat gained by the storage tank is calculated by the energy balance across the primary and secondary and is represented in Fig. 8. The heat the collector gains depends on the heat input insolation values variation concerning time. It depends on other atmospheric factors, such as wind speed, ambient temperature, cloudiness, etc., as Fig. 8(c) represents the Heat input, Energy balance across the collector and the Cumulative heat input of the solar collector.

4.4 Need for Surfactant used in SiO_2 Nanofluid

The SiO_2 nanoparticle is prepared by synthesis of the Chemical Combustion Method particle size of 40 nm. A

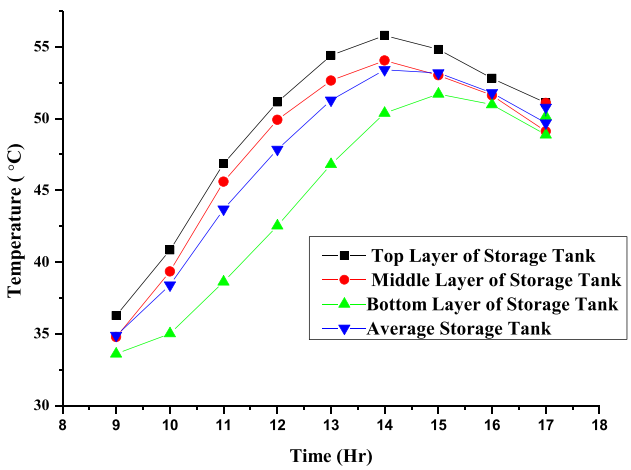

Fig. 7 Temperature variations inside the storage tank

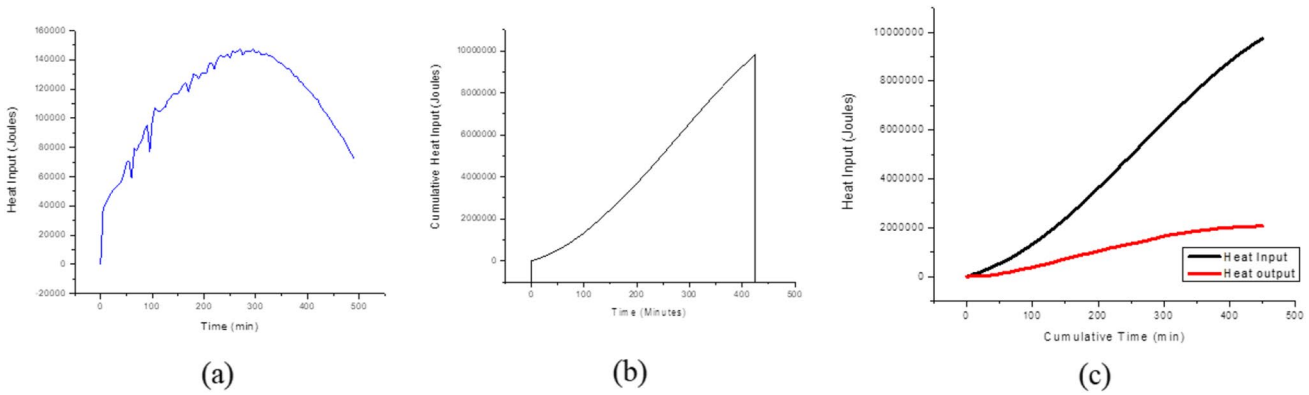

Figure. 8 (**a**) Heat input, (**b**) Energy balance across the collector, (**c**) Cumulative heat input

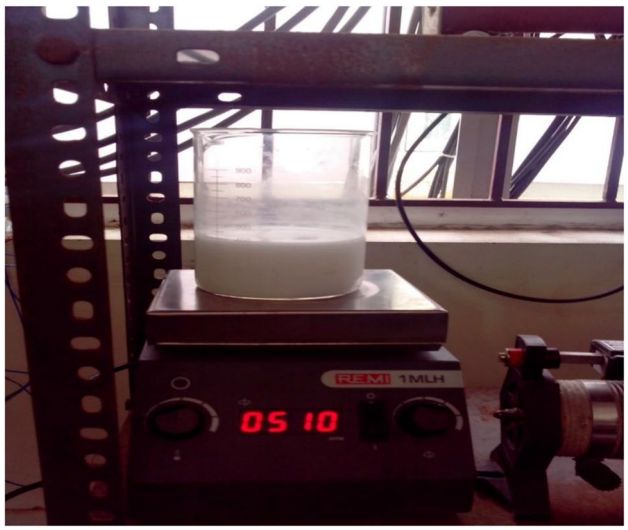

Fig. 9 Magnetic stirrer to ensure uniform dispersion

Nanoparticles of SiO_2 is a prepared sample with 0.2%, 0.4% and 0.8%. The nanoparticles started settling down with different mass fractions of 0.4% and 0.8%. Hence, a surfactant is used to prevent the settling or clumping of Nanoparticles, resulting in better dispersion [32]. A magnetic stirrer is used—Fig. 9 shows a magnetic stirrer for ensuring uniform dispersion. The stability of nanofluids is one factor that prevents their widespread use in solar collectors. This is one of the limiting factors. Nanofluids, in contrast to more traditional working fluids, are extremely unstable, and particles tend to settle out after a while. A decrease in agglomeration within the fluid might be achieved by adjusting the pH, changing the preparation method, or adding a surfactant. Because of the decrease in fluid stability, the overall efficiencies of collector systems continue to decline significantly after lapses of time spanning longer periods [33].

Table 1 Parameters for SiO_2 nanofluid for different weight fraction

Parameters	The volume of distilled water (litre)	Weight fractions (%)	Particle Size (nm)	Thermal conductivity (W/mk)
SiO_2	2.5	0.2	40	0.614
SiO_2	2.5	0.4	40	0.642
SiO_2	2.5	0.8	40	0.676

The KD2 PRO – thermal property analyzer is used to verdict the actual thermal properties of SiO_2 for weight fractions of 0.2%, 0.4% and 0.8% nanofluids

Nanoparticles are compounds that lower the surface tension, the interfacial tension between two liquids, or a liquid and a solid [34]. Dispersants are employed to increase the contact of two materials, sometimes known as wettability. The surfactant used is Cetyl Triammonium Bromide (CTAB) (1% by wt)**.** The mass fraction of SiO_2 nanofluid (with and without surfactant) is operated inside the 25 LPD solar FPC. The following weight fraction is used in the collector. Table 1 shows the parameter for SiO_2 nano-fluids. Figure 10 shows the Scanning Electron Microscope (SEM) image of the SiO_2 nanofluid.

The thermal conductivity of SiO_2 nanofluid increases with an increase in mass fraction. The thermal conductivity of the nanofluid is expected to enhance as the mass fraction increases. This could be attributed to the good dispersion medium of SiO_2 nanofluid [35]. Increasing the mass fraction of SiO_2 nanofluid leads to increasing the Brownian motion, thereby improving the thermal conductivity. Table 1 shows the parameters for SiO_2 Nanofluid for Different Weight Fractions. As can be seen, the obtained results by the current study are in exceptional agreement with the experimental results of other studies [36].

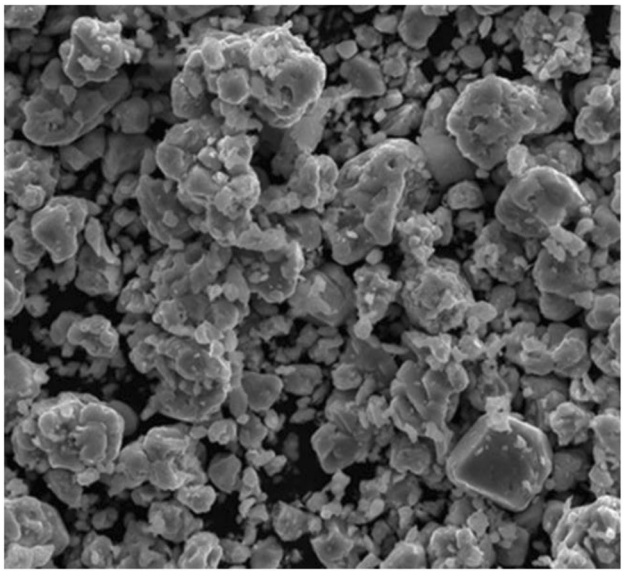

Fig. 10 SEM image of SiO_2

4.5 Temperature Profiles Across the Riser Tubes in the Flat Plate Collectors

The experiment was conducted with water and SiO_2 nanofluid with different weight fractions, and its result is discussed in detail. The temperature profile of collectors at different locations are noted and compared with the nanofluid operation. The temperature change at the inlet and outlet of the primary side of the collector is observed as 7℃. From this temperature profile, for a given collector tube, the flow distribution in tubes at different lengths is observed that flow in all the tubes shows the same temperature change at the same length. Figure 11 shows that the flow distribution is uniform in all the tubes; high tube surface temperature indicates less flow in that tube.

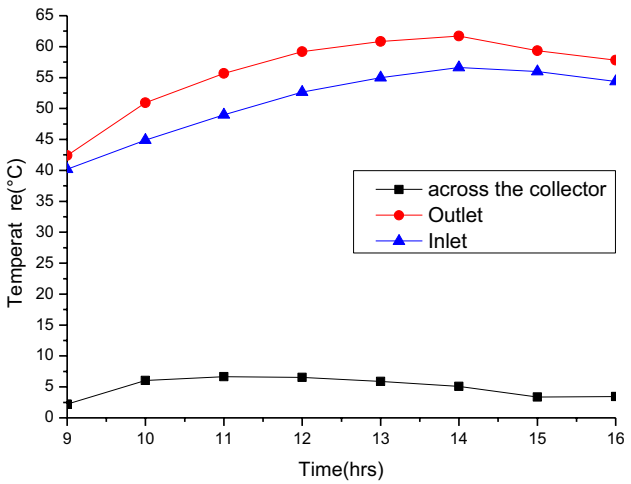

Fig. 11 Temperature profiles across the riser tubes in flat plate collectors

4.6 Temperature Profile of Secondary (Collector) Side with and without Surfactant of SiO_2 Nanofluid

With the rise of the solar insolation, the storage tank temperature gradually rises in all cases (i.e., for different weight fractions of nanofluid) when Silicon dioxide nanoparticles of 0.2%, 0.4% and 0.8% weight fractions are mixed with 2.5 L of distilled water separately is used in 25 LPD collector. Its temperature variation with and without surfactant is operated. When Silicon dioxide of 0.8% is used, the temperature difference is about five °C rises compared to water. It was observed that the temperature started dropping after the time 3 pm. This is due to the loss of thermosphoning effect at lower insolation and the heat input by the absorber plate [37]. This phenomenon happens around 3 pm daily because the insolation decreases during this instant. The collector is operated with nanoparticles of SiO_2 with a particle size of 40 nm nanofluid as a working fluid. Its average tank temperature is compared to the water's conventional working fluid. The temperature changes concerning time and cumulative heat input (Insolation) is indicated that for attaining 50℃, SiO_2 of 0.8% weight fraction reached quickly as compared to that of base fluid, from the experimental result shows (Fig. 12), the temperature rise is faster in case of increase in weight fractions SiO_2 nanofluid [38]. The ability of SiO_2 nanoparticles used in collectors to maximize the absorption rate of the heat received from solar radiation, achieving instant temperature rise. Temperature rise increases with weight fraction and is higher than water owing to the presence of SiO_2 nanoparticles, which acts as a positive characteristic of nanofluids [39].

Also, graphs indicate a 0.2wt%. SiO_2 nanoparticles without surfactants show lesser temperature values. The reason is

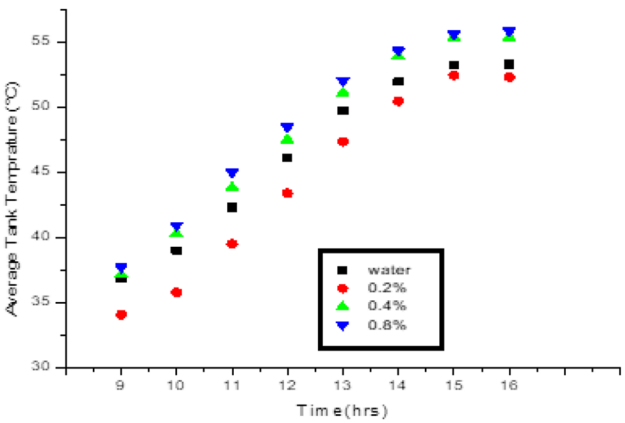

Fig. 12 Temperature variation with and without surfactant

mainly their non-stability of particle dispersion in the water. Also, it has been suggested that non-addition of the surfactant to the SiO_2 nanoparticles, even for a lesser mass fraction, results in poor dispersion, resulting in lesser efficiency when used in a solar collector. As can be seen, the obtained results by the current study are in exceptional contract with the experimental results of other studies [39, 40].

4.7 Efficiency Comparison for Different Weight Fractions of Different Working Fluids

Efficiency is calculated by plotting the weight fractions of SiO_2 nanofluid with surfactant for 8gm and 10gm with the base conventional working fluid water. For a higher mass fraction of SiO_2 (0.8%) nanofluid, higher efficiency was attained in a more rapid phase than SiO_2 (0.4%) nanofluid and water. Also, insolation decreases the thermosyphon effect breaks in the collector during the off-peak time. It was inferred that adding SiO_2 nano-fluids would result in greater efficiency even during the peak time. In contrast, the efficiency decreases in water because the SiO_2 nanofluid has a better heat transfer rate than water. The peak efficiency has arrived or 0.8% SiO_2 nanofluids. Figure 13 shows Efficiency Comparisons for Different Weight Fractions of SiO_2Nanoparticle and water. Table 2 shows the efficiency comparison of different nanofluids and water.

Adding SiO_2 nanoparticles with base fluid enhances the heat transfer rate to the collector system's primary (collector) and secondary side (storage). Further, by adding SiO_2 nanoparticles, the loss of heat transfer in (convective) is minimized, increasing the system's efficiency, as observed in the figure. The collector's efficiency is found to increase with the increase in the mass fraction of SiO_2 nanoparticles [39]. The SiO_2 nanoparticle concentration plays a vital role in determining heat transfer from solar irradiation to the system. The higher the volume percentage of SiO2 nanoparticles, the higher the system's efficiency. A higher concentration of SiO_2 nanoparticles minimizes the pressure drop of the working fluid, enhancing the flow rate and heat transfer. As can be seen, the obtained results by the current study are in exceptional contract with the experimental results of other studies [38–43].

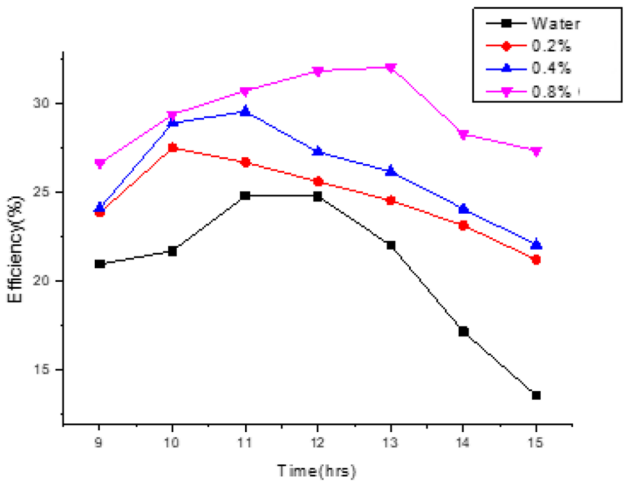

Fig. 13 Efficiency Comparisons for Different Weight Fractions of SiO_2 Nanoparticle and water

5 Conclusion

This work reveals a detailed study on the effect of silica nanoparticles on the performance parameters of the solar water heater. Silicon nanoparticles are dispersed with water to accelerate the vaporization and heating of the medium by local nanoscale heating. A 25-LPD solar collector was designed theoretically and experimentally. Water is fixed as a baseline to compute the overall performance and different parameters for the thermal storage of the tank. A further test was conducted by adding SiO_2 nanofluids with and without surfactant. Dimethyldichlorosilane was employed to prepare silica nanoparticles into hydrophobic nanoparticles. The effect of SiO_2 nanoparticles was analyzed at three different weight proportions. Increasing the gravimetric percentage of nanoparticles improved the efficiency of SFPWHS. The SiO_2 nanofluid at different mass fractions increased the overall efficiency with the same collector area and without an increase in mass flow rate, considerably lowering the capital cost. The efficiency of the solar collector at weight fractions of 0.2%, 0.4% and 0.8% of the Silicon dioxide nanoparticles and water was found to be 26.7, 29.3, 33.7% and 24.2%, respectively. SiO_2 nanofluid beyond 0.8% mass fractions affects the thermosiphon principle during natural convection

Table 2 Efficiency comparison of different nanofluids and water

Working fluid	The weight fraction of nanofluid	Particle Size (nm)	The volume of the primary circuit	The volume of sec. circuit	Efficiency (%)
Water	–	–	2.5	25	24.2
SiO_2	0.2%	40	2.5	25	26.7
SiO_2	0.4%	40	2.5	25	29.33
SiO_2	0.8%	40	2.5	25	33.7

pressure drop, affecting the system's overall thermal performance. Thus this study concludes that the SiO_2 nanofluid would be a better option for better longevity as a working fluid to enhance the collector's performance.

Credit Authorship Contribution Statement Dinesh babu Munuswamy: Methodology, Validation, Formal analysis, Investigation, Writing an original draft, Review & editing, Visualization. Yuvarajan Devarajan: Resources, Supervision, Funding acquisition, Writing – review & editing.

Data Availability The data sources used in this Research are accessible upon proper request from the corresponding author.

Many authors practise no investigations with human participants or animals in this article.

Declarations

Consent to Participate Not applicable.

Consent for Publication Not applicable.

Competing Interest The authors proclaim that they have no known competing financial interests or personal relationships that could have influenced the Research presented in this paper.

References

1. Subramanian B, Lakshmaiya N, Ramasamy D, Devarajan Y (2022) Detailed analysis on engine operating in dual fuel mode with different energy fractions of sustainable HHO gas. Environ Prog Sustain Energy e13850. https://doi.org/10.1002/ep.13850
2. Tiwari R, Kumar R (2021) Analysis of plane wave propagation under the purview of three phase lag theory of thermoelasticity with non-local effect. Eur J Mech A Solids 88:104235. https://doi.org/10.1016/j.euromechsol.2021.104235
3. Tiwari R, Kumar R, Abouelregal AE (2021) Analysis of a magneto-thermoelastic problem in a piezoelastic medium using the non-local memory-dependent heat conduction theory involving three phase lags. Mech Time-Dep Mater. https://doi.org/10.1007/s11043-021-09487-z
4. Tiwari R, Misra JC, Prasad R (2021) Magneto-thermoelastic wave propagation in a finitely conducting medium: A comparative study for three types of thermoelasticity I, II, and III. J Therm Stress 44(7):785–806. https://doi.org/10.1080/01495739.2021.1918594
5. Tiwari R (2021) Magneto-thermoelastic interactions in generalized thermoelastic half-space for varying thermal and electrical conductivity. Waves Random Complex Media 1–17. https://doi.org/10.1080/17455030.2021.1948146
6. Matheswaran MM, Arjunan TV, Muthusamy S, Natrayan L, Panchal H, Subramaniam S, Khedkar NK, El-Shafay AS, Sonawane C (2022) A case study on thermo-hydraulic performance of jet plate solar air heater using response surface methodology. Case Stud Therm Eng 34:101983. https://doi.org/10.1016/j.csite.2022.101983
7. Rostami S, Hamid ASA, Sopian K, Jarimi H, Bassim A, Ibrahim A (2022) Heat Transfer Analysis of the Flat Plate Solar Thermal Collectors with Elliptical and Circular Serpentine. Tube Appl Sci 12:4519. https://doi.org/10.3390/app12094519
8. Khimsuriya YD, Patel DK, Said Z, Panchal H, Jaber MM, Natrayan L, Patel V, El-Shafay AS (2022) Artificially roughened solar air heating technology-a comprehensive review. Appl Therm Eng 118817. https://doi.org/10.1016/j.applthermaleng.2022.118817
9. Abu-Hamdeh NH, Alazwari MA, Salilih EM, Sajadi SM, Karimipour A (2021) Improve the efficiency and heat transfer rate' trend prediction of a flat-plate solar collector via a solar energy installation by examine the Titanium Dioxide/Silicon Dioxide-water nanofluid. Sustain Energy Technol Assess 48:101623
10. Farhana K, Kadirgama K, Mohammed HA, Ramasamy D, Samykano M, Saidur R (2021) Analysis of efficiency enhancement of flat plate solar collector using crystal nano-cellulose (CNC) nanofluids. Sustain Energy Technol Assess 45:101049
11. Ramesh C, Vijayakumar M, Alshahrani S, Navaneethakrishnan G, Palanisamy R, Natrayan L, Saleel CA, Afzal A, Suboor S, Panchal H (2022) Performance enhancement of selective layer coated on solar absorber panel with reflector for water heater by response surface method: a case study. Case Stud Therm Eng 36:102093. https://doi.org/10.1016/j.csite.2022.102093
12. Ahmadi A, Ehyaei MA, Doustgani A, Assad MEH, Hmida A, Jamali DH, Kumar R, Li ZX, Razmjoo A (2020) Recent Residential Applications of low-temperature solar collector. J Clean Prod 279:123549. https://doi.org/10.1016/j.jclepro.2020.123549
13. Gorjian S, Ebadi H, Calise F, Shukla A, Ingrao C (2020) A review on recent advancements in performance enhancement techniques for low-temperature solar collectors. Energy Convers Manag 222:113246. https://doi.org/10.1016/j.enconman.2020.113246
14. Munuswamy DB, Devarajan Y, Ramalingam S, Subramani S, Munuswamy NB (2022) Critical review on effects of alcohols and nanoadditives on performance and emission in low-temperature combustion engines: advances and perspectives. Energy Fuel. https://doi.org/10.1021/acs.energyfuels.2c00930
15. Hussein OA, Habib K, Muhsan AS, Saidur R, Alawi OA, Ibrahim TK (2020) Thermal performance enhancement of a flat plate solar collector using hybrid nanofluid. Sol Energy 204:208–222. https://doi.org/10.1016/j.solener.2020.04.034
16. Moravej M, Bozorg MV, Guan Y, Li LKB, Doranehgard MH, Hong K, Xiong Q (2020) Enhancing the efficiency of a symmetric flat-plate solar collector via the use of rutile TiO2-water nano-fluids. Sustain Energy Technol Assess 40:100783. https://doi.org/10.1016/j.seta.2020.100783
17. Mohamed MM, Mahmoud NH, Farahat MA (2020) Energy storage system with flat plate solar collector and water-ZnO nanofluid. Sol Energy 202:25–31. https://doi.org/10.1016/j.solener.2020.03.060
18. Tong Y, Chi X, Kang W, Cho H (2020) Comparative investigation of efficiency sensitivity in a flat plate solar collector according to nanofluids. Appl Therm Eng. https://doi.org/10.1016/j.applthermaleng.2020.115346
19. Munuswamy DB, Devarajan Y, Babu MN, Ramalingam S (2020) Experimental investigation on lowering the environmental hazards and improving the performance patterns of solar flat plate collectors by employing the internal longitudinal fins and nano additives. Environ Sci Pollut Res. https://doi.org/10.1007/s11356-020-10311-3
20. Devarajan Y, Jayabal R, Munuswamy D, Ganesan S, Varuvele EG (2022) Biofuel from leather waste fat to lower diesel engine emissions: valuable Solution for lowering fossil fuel usage and perception on waste management. Process Saf Environ Prot. https://doi.org/10.1016/j.psep.2022.07.001
21. Mondragon R, Sanchez D, Cabello R, Llopis R, Julia JE (2019) Flat plate solar collector performance using alumina nanofluids: experimental characterization and efficiency tests. PLoS ONE. https://doi.org/10.1371/journal.pone.0212260

22. Tong Y, Lee H, Kang W, Cho H (2019) Energy and exergy comparison of a flat plate solar collector using water, Al_2O_3 nanofluid, and SiO2 nanofluid. Appl Therm Eng. https://doi.org/10.1016/j.applthermaleng.2019.113959
23. Mirzaei M (2019) Experimental investigation of SiO2 nanofluid in the thermal characteristics of a flat plate solar collector. Environ Prog Sustain Energy. https://doi.org/10.1002/ep.12902
24. Arora S, Fekadu G, Subudhi S (2019) Energy and exergy analysis of Marquise shaped channel flat plate solar collector using Al_2O_3-water nanofluid and water. J Solar Energy Eng Trans ASME. https://doi.org/10.1115/1.4042454
25. Dehaj MS, Mohiabadi MZ (2019) Experimental investigation of heat pipe solar collector using MgO nano-fluids. Sol Energy Mater Sol Cells. https://doi.org/10.1016/j.solmat.2018.10.025
26. Devarajan Y, Nagappan B, Subbiah G et al (2021) Experimental investigation on solar-powered ejector refrigeration system integrated with different concentrators. Environ Sci Pollut Res 28:16298–16307. https://doi.org/10.1007/s11356-020-12248-z
27. Mirzaei M, Hosseini SMS, Moradi Kashkooli AM (2018) Assessment of Al_2O_3 nanoparticles for the optimal operation of the flat plate solar collector. Appl Therm Eng. https://doi.org/10.1016/j.applthermaleng.2018.01.104
28. Syam Sundar L, Kirubeil A, Punnaiah V, Singh MK, Sousa ACM (2018) Effectiveness analysis of solar flat plate collector with Al2O3 water nanofluids and with longitudinal strip inserts. Int J Heat Mass Transfer. https://doi.org/10.1016/j.ijheatmasstransfer.2018.08.025
29. Jouybari HJ, Saedodin S, Zamzamian A, Nimvari ME, Wongwises S (2017) Effects of porous material and nanoparticles on the thermal performance of a flat plate solar collector: an experimental study. Renew Energy. https://doi.org/10.1016/j.renene.2017.07.008
30. Stalin PMJ, Arjunan TV, Matheswaran MM, Sadanandam N (2017) Experimental and theoretical investigation on the effects of lower concentration CeO2/ water nanofluid in flat-plate solar collector. J Therm Anal Calorim 135:1–16. https://doi.org/10.1007/s10973-017-6865-4
31. Munuswamy DB, Devarajan Y (2016) Analysis on the Influence of Nanoparticles of Alumina, Silicon dioxide, and Zirconium Oxide on the Performance of a Flat-Plate Solar Water Heater. Energy Fuels 30(11):9908–9913
32. Munuswamy DB, Devarajan Y, Naresh Babu M (2020) Experimental investigation on lowering the environmental hazards and improving the performance patterns of solar flat plate collectors by employing the internal longitudinal fins and nano additives. Environ Sci Pollut Res 27:45390–45404
33. Faizal M, Saidur R, Mekhilef S, Hepbasli A, Mahbubul IM (2015) Energy, economic, and environmental analysis of a flat-plate solar collector operated with SiO2 nanofluid. Clean Technol Environ Policy. https://doi.org/10.1007/s10098-014-0870-0
34. Munuswamy DB, Madhavan VR, Mohan M (2015) Comparison of the effects of Al_2O_3 and CuO nanoparticles on the performance of a solar flat-plate collector. J Non-Equilibrium Thermodyn 40(4):265–273
35. Beemkumar N, Dinesh Kumar S, Dhass AD, Yuvarajan D, Krishna Kumar TS (2021) Impact on the Performance of Solar Photovoltaic System with the Innovative Cooling Techniques. In: Motahhir S, Eltamaly AM (eds) Advanced Technologies for Solar Photovoltaics Energy Systems. Green Energy and Technology. Springer, Cham. https://doi.org/10.1007/978-3-030-64565-6_5
36. Lacroix M (1993) study of the heat transfer behavior of a latent heat thermal energy storage unit with a finned tube. Int J Heat Mass Transf 36:2083–2092
37. Beemkumar N, Yuvarajan D, Arulprakasajothi M, Ganesan S, Elangovan K, Senthilkumar G (2019) Experimental Investigation and Numerical Modeling of Room Temperature Control in Buildings by the Implementation of Phase Change Material in the Roof. J Solar Energy Eng 142(1). https://doi.org/10.1115/1.4044564
38. Sheik MA, Aravindan MK, Beemkumar N et al (2022) Enhancement of heat transfer in PEG 1000 using nano-phase change material for thermal energy storage. Arab J Sci Eng. https://doi.org/10.1007/s13369-022-06810-9
39. Beemkumar N, Yuvarajan D, Arulprakasajothi M, Elangovan K, Arunkumar T (2020) Control of room temperature fluctuations in the building by incorporating PCM in the roof. J Therm Anal Calorim. https://doi.org/10.1007/s10973-019-09226-0
40. Nagappan B, Devarajan Y, Kariappan E (2022) Performance analysis of sustainable solar energy operated ejector refrigeration system with the combined effect of Scheffler and parabolic trough collectors to lower greenhouse gases. Environ Sci Pollut Res 29:48411–48423. https://doi.org/10.1007/s11356-022-19058-5
41. Vijayaragavan M, Subramanian B, Sudhakar S, Natrayan L (2021) Effect of induction on exhaust gas recirculation and hydrogen gas in compression ignition engine with simarouba oil in dual fuel mode. Int J Hydrog Energy. https://doi.org/10.1016/j.ijhydene.2021.11.201
42. Muthiya SJ, Natrayan L, Yuvaraj L, Subramaniam M, Dhanraj JA, Mammo WD (2022a) Development of active CO2 emission control for diesel engine exhaust using amine-based adsorption and absorption technique. Adsorpt Sci Technol 2022:1–8. https://doi.org/10.1155/2022/8803585
43. Muthiya SJ, Natrayan L, Kaliappan S, Patil PP, Naveena BE, Dhanraj JA, Subramaniam M, Paramasivam P (2022b) Experimental investigation to utilize adsorption and absorption technique to reduce CO2 Emissions in diesel engine exhaust using amine solutions. Adsorpt Sci Technol 2022:1–11. https://doi.org/10.1155/2022/9621423